Equivalent Network Approach for the Simulation of MEMS Devices

S. Barmada, A. Musolino, R. Rizzo

Department of Electric Systems and Automation, University of Pisa
Via Diotisalvi n.2, 56126 Pisa, Italy
{sami.barmada, musolino, rocco.rizzo}@dsea.unipi.it

Abstract: In this paper a numerical approach for the analysis of the behaviour of micro electro mechanical systems (MEMS) is presented. The method is applied to the simulation of movable plate MEMS variable capacitors that are of common use in the CMOS voltage controlled oscillators (VCOs). An accurate study of MEMS devices requires a coupled electro-mechanical analysis. The mechanical analysis has to take into account the deformation of the plates of the capacitor and the electromagnetic one has to consider the distribution of charges and currents and the presence of dielectric materials.

We first perform a coupled elastic-electrostatic analysis in order to obtain the tuning characteristic of the system; subsequently, once the positions of the plates have been determined, an electromagnetic analysis of the system is performed via an integral formulation based on an electric equivalent circuit.

The proposed method has been validated by analysing two and three plate tuneable parallel-plate capacitors.

Keywords: Integral Formulations, Method of Moments, MEMS, Finite Element Method.

1   Introduction

Micro Electro Mechanical System (MEMS) is a technology able to produce miniature mechanical structures, devices and systems by the use of the state of the art of integrate circuit (IC) fabrication [1] - [3]. The advantages inherited by IC technology are mainly the cost reduction (through batch fabrication) and the opportunity of the dimensional downscaling. As a consequence of the latter, the power consumption has been decreased with an important improvement of the overall performance. The mechanical property of silicon has given the opportunity of the fabrication of MEMS by compatible materials with the IC technology. This has led to the realization of monolithic integrated electromechanical systems including accelerometers, pressure sensors and micro switches.

When used as radio frequency (RF) components MEMS devices are showing great potentialities. They demonstrate higher linearity and lower loss than similar components built by other technologies. In this perspective RF MEMS, such as RF switches, tuneable capacitors and high-Q inductors, may serve as fundamental building blocks and are becoming more and more used in several critical applications where increased functionality has to be conjugated with reduced power consumption and severe constraints of electromagnetic compatibility [3] - [5].

As an example it is sufficient to consider modern communication systems, such as the GSM cellular telephone system, where stringent requirements on the intermediate filters and on the VCOs are present. In particular the dynamic range of the filters and the noise level of a RF VCO depend (in opposite fashion) on the overall Q-factor of the resonator.

A proper design procedure for these devices depends on an accurate analysis of the resonator whose tuneable component can be advantageously realized by a MEMS capacitor [6] – [8]. Unbiased base capacitance, tuning ratio, quality factor, associated inductance and consequent electric self resonance frequency are figures of merit of current use in association with tunable capacitors. Their evaluation requires a deep analysis of the device. The long computation times usually required by full wave coupled analysis result in the introduction of approximations with consequent inaccurate predictions producing an unacceptable design process through trial and error.

A MEMS simulator should be able to perform a coupled electro-mechanical analysis [4], [5], [9]. The rigid-body motion hypothesis of the movable plate is no longer valid because of the high width to thickness ratio. The deformations of the moving plate may heavily affect the overall performance of the system as the effective stiffness of the system decreases and as a consequence the mechanic self resonant frequency and the pull-in voltage decrease as well. The accurate determination of the electrical figures of merit of MEMS tunable capacitors requires the evaluation of the charge and current distributions. Fringing effects and the presence of dielectric materials influence the values of the capacity at the various bias levels; the effective distribution of the currents in the device determines the

actual ohmic losses that, in conjunction with the dielectric losses, are used to evaluate the quality factor. A correct evaluation of the quality factor has to take into account the inductive effects of the currents influencing the overall reactance of the system at a given frequency. In addition the evaluation of the inductive effects is essential in the calculation of the electric self resonant frequency.

The mechanic self resonant frequency of a MEMS capacitor usually lies in the range $10 \div 100 \, KHz$ while the RF signal is in the range $0.1 \div 10 \, GHz$. The RF frequencies are at least three orders of magnitude of mechanical bandwidth; as known this wide separation allows a simplified electromechanical coupling. The position and the deformations of the moving plate are unlikely to be caused by the RF signal and may be determined as a function of the bias voltage only. At the corresponding low frequencies the charge distribution and the electric field play a dominant role in the evaluation of the force distribution. The system in the new geometric configuration so determined is considered at rest under the effects of the RF signal.

This paper discusses various aspects of a method for the electromagnetic analysis based on an integral formulation via an equivalent network.

Conductors and dielectrics (assumed linear) are subdivided in elementary volumes in which uniform distributions of current density and electric polarization are assumed. Ohm's law and continuity equation for the current are written for conductive materials; these are coupled with the constitutive equation for the dielectrics leading to a set of equations that can be viewed as the equilibrium equations of an electric network.

The knowledge of the currents, charges and distribution of the polarization allows evaluating the most important figures of merit of the device.

2   Formulation

As stated in the introduction two analyses have to be performed on a MEMS device: first a coupled electromechanical analysis and subsequently an electromagnetic one.

The first one is a fully three-dimensional analysis that iterates between a mechanical Finite Element Method (FEM) solution and an electrostatic Method Of Moment (MOM) solution.

The second one is purely electromagnetic and uses results and parameters obtained by the former.

The electromechanical analysis is explained in detail in the literature and it will be summarized with the objective to define the parameters that will be exported to the electromagnetic analysis.

Let us consider a system constituted by a conductor and by a linear dielectric body. The system is discretized in elementary volumes (slabs, cylindrical sectors of rectangular cross section).

Let N_d be the number of the elementary volumes resulting by the discretization of the dielectric bodies, and N_c the number of the elementary conductive volumes. A uniform distribution of the polarization is assumed in each dielectric elementary volume.

2.1   Electro-mechanical Analysis

The discretization of the conductive body produces a discretization of the surface of the body itself in N_s elementary surface elements. Let us assume a uniform distribution of the charges on these surface elements.

The deformable regions (i.e. the moving plate), where a mechanical FEM is used, are further meshed according with the used structural analysis software [10].

Two meshes are defined on the same region: the first one is used to evaluate the force, the second one to calculate the displacements and the deformations.

The force distribution on the moving plate can be evaluated once the charge and polarization distribution are known.

Because of the assumed uniform distribution of the electrical quantities we can write the following expression for the electric scalar potential:

$$\varphi(P) = \frac{1}{4\pi\varepsilon_0} \sum_{j=1}^{N_S} \int_{S_{j,cond}} \frac{\sigma_j(Q)}{r_{P,Q}} dQ + \frac{1}{4\pi\varepsilon_0} \sum_{j=1}^{N_d} \int_{S_{j,pol}} \frac{P_j(Q) \cdot n}{r_{P,Q}} dQ =$$
$$= \sum_{j=1}^{N_S} \alpha_{P,j} \, \sigma_j + \sum_{j=1}^{N_d} \beta_{P,j} \cdot P_j \, .$$

(1)

In the above expression $\alpha_{P,j}$ represents the potential in P due to a charge uniformly distributed with unit density on the jth elementary surface of a conductor; the vector $\beta_{P,j}$ relates the electric potential in P to the jth elementary volume where a uniform polarization is assumed. In the second integral in (1) $S_{j,pol}$ represents the entire surface of the jth elementary volume resulting by the discretization of the dielectric regions.

A similar expression can be derived for the electric field at P:

$$E(P) = -\nabla\varphi(P) = \sum_{j=1}^{N_S} \delta_{P,j} \, \sigma_j + \sum_{j=1}^{N_d} \Theta_{P,j} \, P_j \, . \qquad (2)$$

The meaning of the symbols in (2) is easily understood: $\delta_{P,j}$ is a vector column and $\Theta_{P,j}$ is a second order tensor represented by a square matrix. The coefficients

$\alpha_{P,j}$, $\beta_{P,j}$, $\delta_{P,j}$, and $\Theta_{P,j}$ can be quickly and accurately evaluated by means of analytical expressions.

The N_s charge densities and the $3N_d$ components of the polarization vector are unknown quantities whose determination is achieved by enforcing the equipotential nature of the conductors and the constitutive equation of dielectrics.

Let ε_r be the relative permittivity of the linear dielectric materials. We write the relation between $\boldsymbol{P}$, $\boldsymbol{E}$, and $\boldsymbol{D}$ inside the ith dielectric elementary volume:

$$\boldsymbol{D}_i = \varepsilon_0 \boldsymbol{E}_i + \boldsymbol{P}_i . \tag{3}$$

Substituting it in the constitutive equation of the material $\boldsymbol{D} = \varepsilon_r \varepsilon_0 \boldsymbol{E}$ yields:

$$\boldsymbol{P}_i (P) = \varepsilon_0 (\varepsilon_r - 1) \boldsymbol{E}_i (P) . \tag{4}$$

Equation (4) is enforced by using the Galerkin procedure at every dielectric elementary volume [11]:

$$\boldsymbol{P}_i = \varepsilon_0 (\varepsilon_r - 1) \left(\sum_{j=1}^{N_S} \delta_{i,j} \sigma_j + \sum_{j=1}^{N_d} \Theta_{i,j} \boldsymbol{P}_j \right) \quad i = 1,..,N_d \tag{5}$$

and the result is projected along the reference axes.

In the usual operation the bias voltage of every conductor with respect to an arbitrarily chosen reference conductor is known. Galerkin method is used to enforce the equipotential nature of the conductors. If a proper numbering of the elementary surfaces is performed (the indexes of the surfaces of a conductors are contiguous), we can write:

$$V_k = \sum_{j=1}^{N_S} \alpha_{k,j} \sigma_j + \sum_{i=1}^{N_d} \beta_{k,i} \cdot \boldsymbol{P}_i , \qquad k = 1,..,N_s . \tag{6}$$

The terms V_k s have to be constant if the elementary surfaces identified by the index k are on the same (equipotential) conductor.

The coefficients $\delta_{i,j}$, $\Theta_{i,j}$, $\alpha_{k,j}$, and $\beta_{k,j}$ in eqs. (5) and (6) are obtained by the corresponding ones in eqs. (1) and (2) by averaging them on the ith dielectric elementary volume and on the kth elementary surface [12].

Once the linear algebraic system formed by eqs. (5) and (6) is solved (giving the charge and polarization distributions) it is possible to evaluate the force distribution on the moving plate.

The structural analysis software is then able to evaluate the movement and the deformation of the armatures. At this newly evaluated geometric configuration we have to repeat the above described electrostatic analysis. A new force distribution is evaluated and the structural

analysis is again performed. Usually a reduced number of iterates are necessary to reach the convergence.

2.2   Electromagnetic Analysis

In the most general case the deformed geometry cannot be discretized by using slabs and cylindrical sectors of rectangular cross section. General hexahedral elements are needed. The described analysis can be performed with these volumes but with longer calculation time because of the non availability of fast and accurate analytical expressions for the evaluation of the fields and potentials. Because of the limited extent of the deformations the hexahedra can be "approximated" by slabs with a negligible loss of accuracy and the analytical expressions can still be used.

This same approximation is used in the electromagnetic analysis; the N_c conductive volumes are advantageously considered as slabs or cylindrical sectors of rectangular cross section.

We now consider the centers of the elementary volumes of the discretized conductor and connect the centres of nearby elements (by segments or by circle arches). We also consider the centre of each exterior surface and connect it to the centre of the elementary volume to which it belongs. A 3-D grid is so obtained [13]. The total number of the points of the grid is then: $N_c + N_S$.

We then associate to each segment of the grid a new elementary volume having four edges parallel to the segment and the faces normal to the segment with their centres placed at the nodes of the grid. Inside each elementary volume a uniform distribution of current density $\boldsymbol{J}$ is assumed. This current is directed parallel to the segment above used. Its direction is then perpendicular to the two bases of the new elementary volumes, and is parallel to its lateral surface. These newly built volumes are the branches of the equivalent electric network; let N_b their number. The nodes of this network are the $N_c + N_S$ points introduced above. The procedure is shown in fig. 1.

Let us consider a volume of the original discretization and the associated node; we see that it is located at the centre of an intersection of branches crossing its surfaces. This is shown in the figure 1f. This volume is in the inner part of the conductor and the sum of the currents flowing in the branches leaving the node is zero.

If the node is on the boundary of the conductor, i.e. it is associated to an exterior surface, charges may accumulate on it. The governing equation can be deduced by the continuity equation of the electric current.

(a)   (b)

(c)   (d)

(e)

(f)
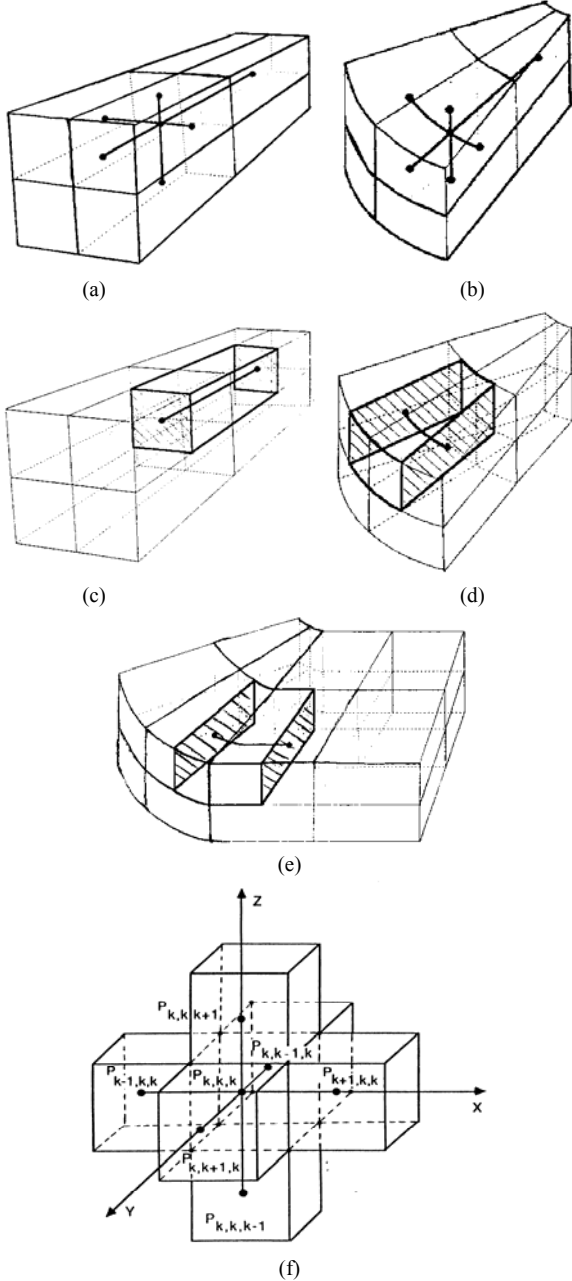
Fig. 1. Construction of the branches of the equivalent network.

Because of the assumed (uniform) distribution of currents and charges we can write:

$$J_{k,h}^{in} = -\frac{\partial \sigma_k^{ext}}{\partial t} \ . \tag{7}$$

In eq. (7) h refers to the node associated with a volume in the inner part of a conductor and k refers to the node associated to an exterior surface. $J_{k,h}^{in}$ and σ_k^{ext} respectively are the current leaving the surface and the charge densities on it.

Because of the assumed distribution of the currents on the branches, the vector potential at a point P can be written as:

$$A(P,t) = \frac{\mu_0}{4\pi} \sum_{j=1}^{N_b} \int_{V_{j,branch}} \frac{J_j(t)}{r_{P,Q}} dQ = \sum_{j=1}^{N_b} \gamma_{P,j} J_j(t) \quad . \tag{8}$$

Let us consider the ith branch and write the Ohm's law at a point P inside it:

$$\rho J(P,t) = E(P,t) = -\nabla \varphi(P,t) - \frac{\partial}{\partial t} A(P,t) \ .$$

Evaluating the line integral along the direction of the current, and averaging the result on the transverse cross section we obtain:

$$R_i I_i(t) = -\Delta U_i(t) - \sum_{j=1}^{N_b} M_{i,j} \frac{d}{dt} I_j(t) \quad , \tag{9}$$

where R_i is the resistance of the ith branch along the direction of the current, $M_{i,j}$ is the coefficient of magnetic coupling with the current of the jth branch and $\Delta U_i(t)$ is the voltages between the terminals of the branch produced by the distribution of charges on the surface of the conductors and by the polarization charges on the dielectrics.

The electromagnetic analysis of the system can be carried on the electric network formed by the interconnection of the N_b branches described by eq. (9). Kirchhoff laws can be used to solve for the currents in this circuit. When the Kirchhoff Current Laws (KCLs) are written at the boundary volumes they assume the form of eq. (7) and the charge densities are added to the set of the unknown branch currents.

Let us now consider a path inside the conductors and write the total voltage along this path; this results in imposing the Kirchhoff Voltage Law (KVL) and the resultant of the $\Delta U_i(t)$s is zero on the closed loops.

The introduction of new unknowns calls for new equations. A relationship has been already obtained involving the charge densities on the surfaces and the voltages between points on the armatures; it is given by the last electrostatic problem solved in iterative procedure used to solve for the coupled electro-mechanical problem. Equations (5) and (6) have to be added to the eqs. (7) and (9).

Before using (5) and (6) we have to consider that at RF the armatures cannot be considered as equipotential regions. As a consequence elementary surfaces lying on the same armature can have different voltages V_k.

We solve eq. (5) in terms of the unknown polarizations of the dielectric elementary volumes expressing them as a linear function of the charge densities:

$$P_i = \sum_{j=1}^{N_S} \lambda_{i,j} \sigma_j, \qquad i = 1,.., N_d . \qquad (10)$$

Substituting in eq. (6) we obtain:

$$V_k = \sum_{j=1}^{N_S} \alpha_{k,j} \sigma_j + \sum_{i=1}^{N_d} \beta_{k,i} \cdot \sum_{j=1}^{N_S} \lambda_{i,j} \sigma_j = \sum_{j=1}^{N_S} \xi_{k,j} \sigma_j, \quad k = 1,.., N_s .$$
$$(11)$$

Performing the inversion we have:

$$\sigma_k = \sum_{j=1}^{N_S} \eta_{k,j} V_j, \qquad\qquad k = 1,.., N_s . \qquad 12)$$

Substituting eq. (12) in (7) we write:

$$J_{h,k}^{in} = -J_{k,h}^{in} = \frac{\partial}{\partial t} \sum_{j=1}^{N_S} \eta_{k,j} V_j, \qquad k = 1,.., N_s . \qquad (13)$$

Equation (13), written at the N_S nodes corresponding to the exterior surfaces, may be viewed as the nodal equilibrium equations of a network. Each node is fed with current generators ($J_{h,k}^{in}$) entering it, and is connected to N_S purely capacitive branches. The reference for the voltages involved in (13) is the external to the circuit and coincides with the reference potential used in the determination of the coefficients $\alpha_{P,j}$ and $\beta_{P,j}$ in eq. (1).

This capacitive network has to be coupled to the network formed by the branches described by eq. (9) connected in correspondence of the N_c nodes associated to the inner elementary volumes. The coupling is performed by observing that the feeding currents of the capacitive subnetwork flow through the impedances built by the procedure described in fig. 1 that connect the centres of the external faces with the centre of the elementary volume they belong to. It is worth to note that these latter impedances are described by eq. (9) too.
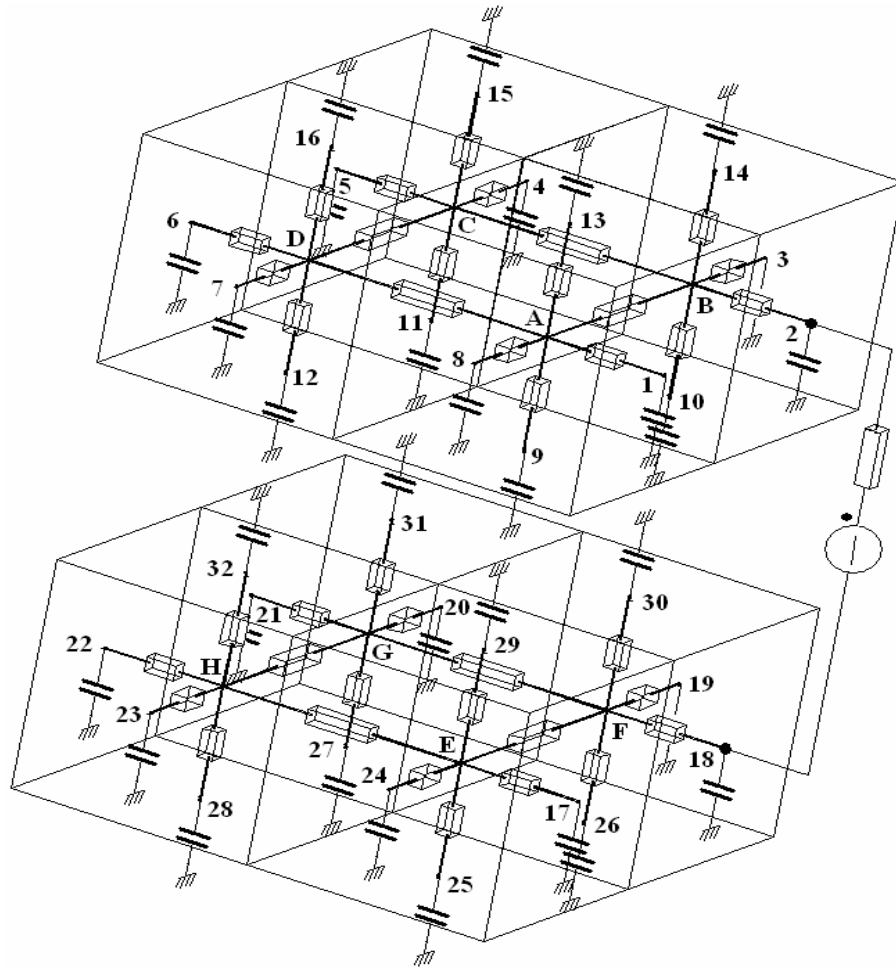
Fig. 2. An example of the equivalent network.

Figure 2 shows an example of the complete equivalent network used for the electromagnetic analysis of a MEMS capacitor in the RF range. A very coarse discretization consisting in four elementary volumes for each armature has been adopted and the system is fed by a voltage generator. For the sake of clarity the capacitors connecting each couple of exterior nodes (those labelled with integer numbers) are not shown; only the capacitors with respect to the reference node of the voltages are indicated. For the same reason the inductive coupling between the impedances is not shown. The nodes labelled with capital letters (A - H) are in the inner of the armature; the nodes labelled with integer numbers (1 - 32) are on the external surfaces. Node A is connected to the inner nodes B and D and to the external nodes 1, 8, 9, and 13.

Modified Nodal Analysis (MNA) can be used to evaluate currents and voltages of the equivalent network. The structure of the network and the "localization" of the inductive coupling mostly in the inner branches and of the capacitive coupling in the exterior ones of the network suggest an "ad hoc" procedure.

Figure 3 shows a simplified version of equivalent network and it is used to illustrate the procedure under the hypothesis of sinusoidal steady state.

Let us consider the subnetworks derived by the armatures; for each subnetwork we can build a surface that cuts the branches connecting the inner with the outer nodes. The capacitors, not shown in fig. 3, are all outside the dashed closed lines that represent the surface in this simplified scheme. Let us label with I_j^b the current on the cut branch directed toward the jth outer node exiting the surface. The total number of these currents is $N_{S_1} + N_{S_2}$, having indicated with N_{S_1} and

N_{S_2} the number of external surfaces of the armature. The portion of network enclosed by these surfaces does not contain capacitors and it is constituted by branches that are magnetically coupled each other.

A mesh analysis of the subnetworks enclosed by the surfaces may be advantageously performed. Let us label the N_m loop currents with I_j^m. The mesh equations written to the central loops of the two subcircuits are:

$$0 = \sum_{j=1}^{N_m} Z_{k,j}^{m,m} I_j^m + \sum_{j=1}^{N_{S_1}+N_{S_2}} Z_{k,j}^{m,b} I_j^b , \quad k = 1, ..., N_m . \quad (14)$$

Superscript m stands for *mesh* and b stands for *branch*. The first superscript in the coefficients $Z_{k,j}^{m,m}$ and $Z_{k,j}^{m,b}$ indicates that we are performing a mesh analysis, the second superscript selects between "*mesh*" or "*branch*" current.

The nodal equations at the nodes outside the surfaces are:

$$I_k^b = \sum_{j=1}^{N_{S_1}+N_{S_2}} Y_{k,j}^{n,n} V_j^n \quad k = 1, ..., N_{S_1} + N_{S_2} ; \ k \neq 6; \ k \neq 22.$$

$$(15a)$$

The equations at node 6 and 22 respectively are:

$$I_6^b = \sum_{j=1}^{N_{S_1}+N_{S_2}} Y_{6,j}^{n,n} V_j^n + I_E^b , \quad (15b)$$

$$I_{22}^b = \sum_{j=1}^{N_{S_1}+N_{S_2}} Y_{22,j}^{n,n} V_j^n - I_E^b , \quad (15c)$$

where I_E^b is the current on the voltage generator directed from node 6 to node 22 and n stands for *nodal*.
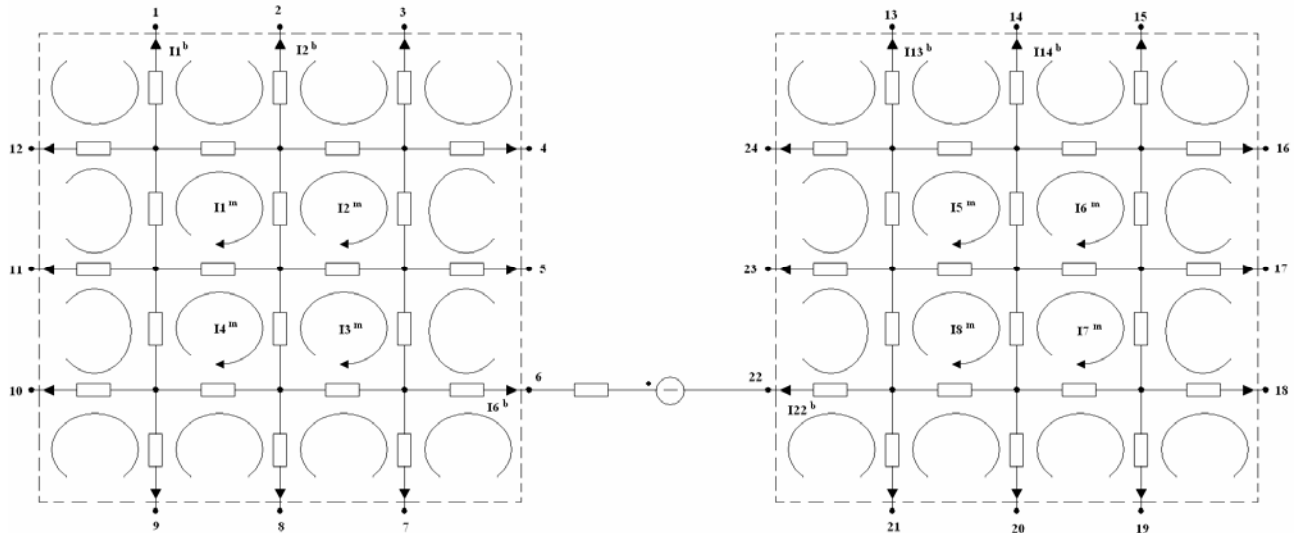
Fig. 3. Simplified equivalent network.

The KCL has to be explicitly imposed on the two closed surfaces:

$$0 = \sum_{j=1}^{N_{S_1}} I_j^b \;, \tag{16a}$$

$$0 = \sum_{j=1+N_{S_1}}^{N_{S_2}} I_j^b \;. \tag{16b}$$

The coupling of the mesh and nodal equations is performed by expressing the voltage between couples of external nodes in terms of the voltage drops along paths that connect the two nodes and that are constituted by branches lying in the inner parts of the subnetworks.
As an example we can write:

$$V_1 - V_2 = \sum_{j=1}^{N_m} Z_{(1,2),j}^{v,m} I_j^m + \sum_{j=1}^{N_{S_1}+N_{S_2}} Z_{(1,2),j}^{v,b} I_j^b \;. \tag{17}$$

The superscript v is for *voltage*; the meaning of the symbols is similar to that of eq. (14). The number of independent paths is $N_{S_1} - 1$ for the first subnetworks and $N_{S_2} - 1$ second one.

A further equation governing the branch with the voltage generator connected to the armatures has to be added,

$$V_6 = Z_E I_E^b + E + V_{22} \;. \tag{18}$$

The total number of the eqs. (14) – (18) is $N_m + 2 \cdot \left(N_{S_1} + N_{S_2} \right) + 1$ and it is the same as the number of the unknown quantities.
By inverting eq. (14) we write:

$$\boldsymbol{I}^m = -\left(\boldsymbol{Z}^{m,m} \right)^{-1} \boldsymbol{Z}^{m,b} \boldsymbol{I}^b \tag{19}$$

where bold characters are used to denote vectors and matrices.
Coupling eqs. (15) and (18) we can write for the voltages at the external nodes the expression:

$$\boldsymbol{V} = \boldsymbol{K} \boldsymbol{I}^b + \boldsymbol{H} \boldsymbol{E} \;. \tag{20}$$

Equation (17) may be written in matrix form by the introduction of the matrix $\boldsymbol{D}$ that performs the difference between two elements of the vector $\boldsymbol{V}$,

$$\boldsymbol{D} \boldsymbol{V} = \boldsymbol{Z}^{v,m} \boldsymbol{I}^m + \boldsymbol{Z}^{v,b} \boldsymbol{I}^b \;. \tag{21}$$

Substituting eqs. (19) and (20) in (21) we obtain:

$$\boldsymbol{D} \left(\boldsymbol{K} \boldsymbol{I}^b + \boldsymbol{H} \boldsymbol{E} \right) = -\boldsymbol{Z}^{v,m} \left(\boldsymbol{Z}^{m,m} \right)^{-1} \boldsymbol{Z}^{m,b} \boldsymbol{I}^b + \boldsymbol{Z}^{v,b} \boldsymbol{I}^b \tag{22}$$

that coupled with eq.(16) allows the evaluation of the currents $\boldsymbol{I}^b$. Back substitution in (19) and (20) completes the solution of the equations.

3 Example of application

Before showing two examples of application let us discuss some properties of the proposed formulation that can be of great usefulness in the analysis of MEMS capacitors.

The typical geometries of the conductive and dielectric domains are characterized by poor aspect ratios. The thickness of the armatures of the capacitor is of the order of micron or less, while the other dimensions are more than two magnitude orders greater. Realistic discretizations of these domains (in terms of number of elementary volumes) result in elementary volumes with very poor aspect ratio. As a consequence the use of analysis tools based on the Finite Element Method (FEM) may result in low accuracy. The proposed formulation belongs to the class of the integral formulations and inherits their properties. In particular the aspect ratio of the elementary volumes produced by the discretization does not affect the accuracy of the computations as in the FEM formulations.

Without appreciable loss of accuracy it is possible to use elementary volumes with poor aspect ratio especially in the central portions of the domains where the polarization vector, the current and the charge densities are likely to be uniformly distributed over relatively large regions. The presence of elementary volumes having one dimension (the thickness) a magnitude order lower than the other two is a common practice in those regions.

The regions near the edges where fringing effects are present may be discretized using elementary volumes "stick" shaped parallel to the edges. The corners and the points where the currents are injected require a finer discretization. This is automatically obtained because of the structured nature of the discretization.

The use of elementary volumes with poor aspect ratio may cause long computation times in the evaluation of the coefficients in eqs. (5) and (6) and of the auto and mutual inductance terms in eq. (9). The availability of analytical expressions for these coefficients mitigates this drawback.

The presence of the holes in the moving armature can be easily modelled and does not result in a dramatic increase of the unknowns because the limited fringing effects in correspondence of the edges of the holes do not require a refinement of the discretization.

Dielectric materials that at RF may present dispersive behaviour with consequent power losses may be easily modelled by the proposed method. A complex frequency dependent electric permittivity in eqs. (4) and (5), when they are written in the frequency domain, implies the presence in eq. (13) of complex $\eta_{k,j}$ coefficients. As a consequence the equivalent network portion built starting from eq. (13) has to be completed by inserting proper resistances parallel connected to the

capacitors already inserted. If a transient analysis has to be performed convolution integrals appear in the equilibrium equations and long computational time may be required unless the dispersive medium is a Lorentz or Debye one [14].

The reduction of the electromagnetic analysis to a network analysis makes very easy the coupling of the MEMS capacitors with the external circuit and allows an accurate, though extremely CPU consuming, analysis of the overall system.

The proposed formulation has been used to analyse two tunable parallel plate capacitors. The complete description of the geometries of the devices is reported in [6]. The principle of operation assumes that the moving plates in both the capacitors behave as rigid bodies, i.e move without deformation. This hypothesis is not valid because of the shape of the plates whose thickness is far less than the other two dimensions. The effective stiffness of the systems is lower than that estimated by considering the stiffness of the T-type suspension only. As a result the pull in voltage and the natural frequency also decrease.

Figures 4 - 6 show the natural frequency versus the bias voltage for the two and three plates MEMS capacitors respectively.
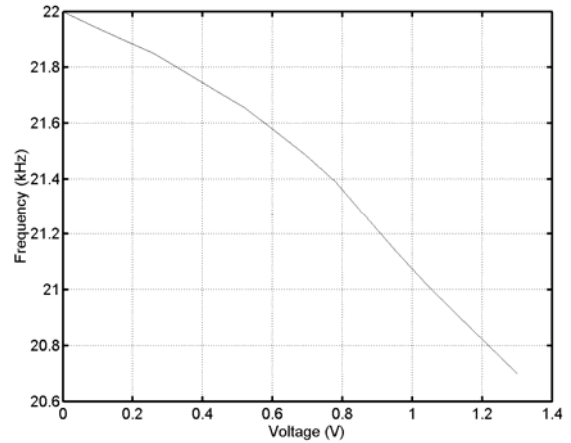
Fig. 6. Three plate capacitor natural frequency vs. V_1 with $V_2=0$.
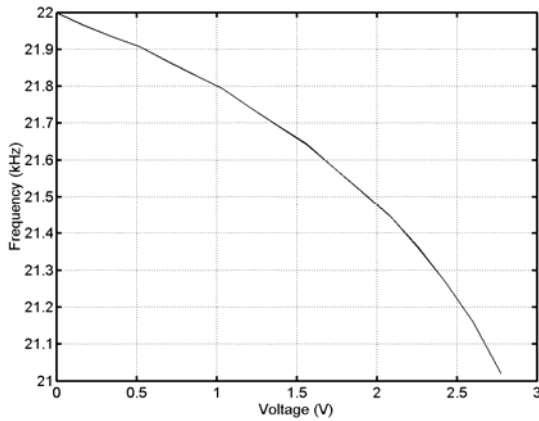
Fig. 4. Two plate MEMS capacitor natural frequency.
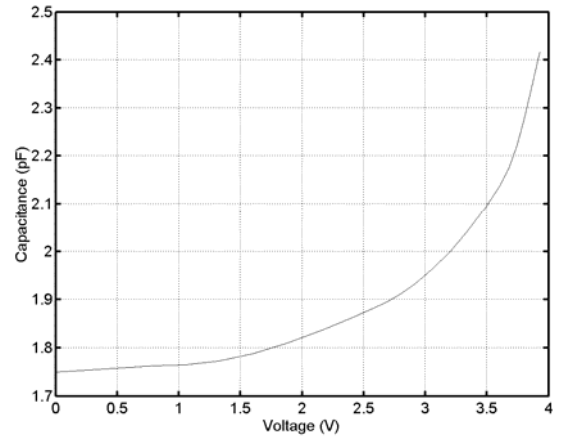
Fig. 7. Tuning characteristics of the two plate capacitor.
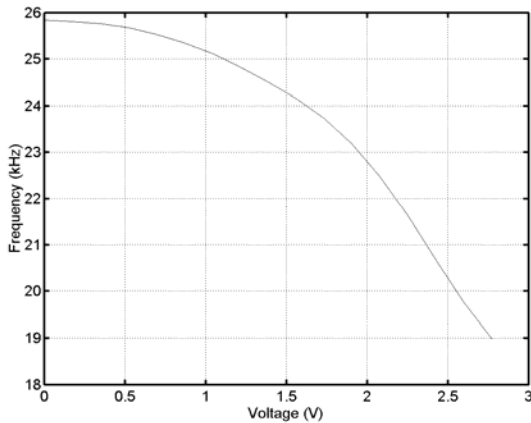
Fig. 5. Three plate capacitor natural frequency vs. V_2 with $V_1=0$.
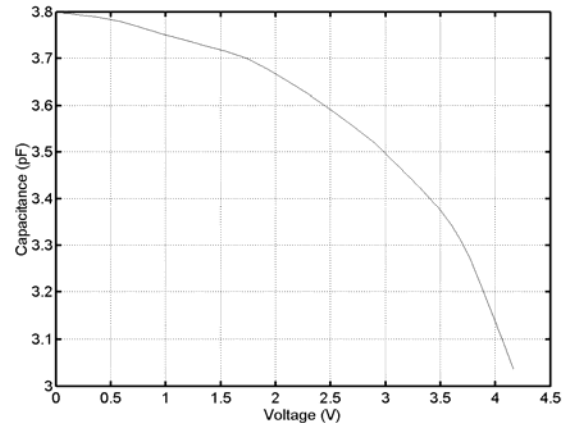
Fig. 8. Tuning characteristics of the three plate capacitor vs. V_2 with $V_1=0$.
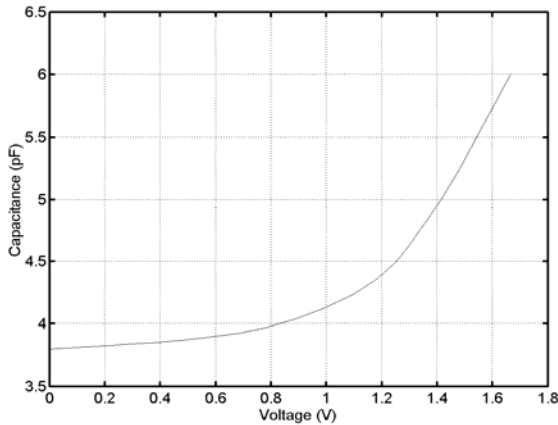
Fig. 9. Tuning characteristics of the three plate capacitor vs. V_1 with V_2=0.

As expected the natural frequencies are smaller than those evaluated in [6] where the rigid motion of the armature is assumed; furthermore a dependence of the natural frequencies with the applied bias voltage is evidenced.

Figure (7) shows the tuning characteristic of the two plate tunable capacitor. The tuning ratio is approximately 1.45 and the pull-in occurs at about 4 V. Figures 8 and 9 show the tuning characteristics of the three plates capacitors with respect to two bias voltages. Figure 8 refers to the voltage between the bottom and the suspended plate, and fig. 9 to the voltage between the top and the moving plate. Pull –in occurs when 4.2 V are applied to the bottom plate and when 1.65 V are applied to the top plate.

All the three simulated tuning characteristics significantly differ from the experimental ones reported in [6]. The cause of these differences is likely due to the effects of the deformations produced by the compressive stress in polysilicon layer that in our analysis has been neglected.
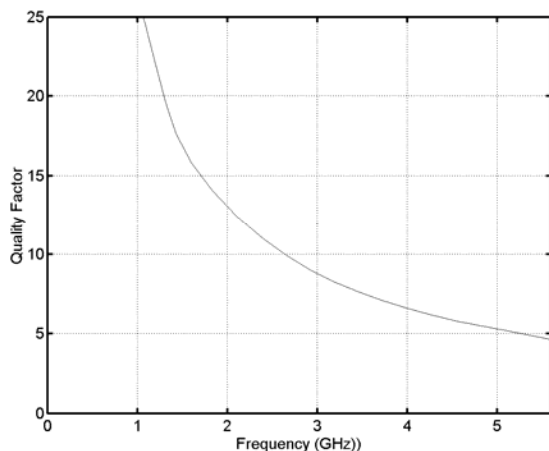
Fig. 10. Simulated "Q" quality factor.

Figure 10 shows the simulated quality factor for the two plate capacitor. A satisfactory agreement with the data reported in [6] is obtained so confirming the ability of the proposed method.

4   Conclusion

In this paper we propose a numerical technique for the simulation of MEMS devices. The method is based on the coupling between electrical and mechanical analysis, taking into account both the deformations and the electromagnetic interactions. A standard FEM structural formulation is coupled with the MoM for the bias analysis; an equivalent network approach based on an integral formulation is used for the electromagnetic analysis and allows to be interfaced with a full wave model of the entire devices.

The method has been tested on a MEMS capacitor, giving consistent results.

References

[1] S. D. Senturia, N. Aluru, J. White, "Simulating the behaviour of MEMS Devices: Computational Methods and Needs," *IEEE Computational Science & Engineering*, pp. 30-43, January – March 1997.

[2] S. D: Senturia, "CAD Challenge for Microsensors, Microactuators, and Microsystems," *Proceedings of the IEEE,* Vol. 86, No. 8, pp. 1611 – 1626, August 1998.

[3] J J. Yao, "RF MEMS from a device perspective," *J. Micromech. Microeng.* 10, pp. 9-38, 2000.

[4] N. Bushyager, B. McGarvey, E. M. Tentzeris, " Introduction of an Adaptive Modeling Technique for the Simulation of RF Structures Requiring the Coupling of Maxwell's, Mechanical, and Solid – State Equations," *ACES Journal*, Vol 17, No. 1 pp. 104-111, March 2002.

[5] M. Kuroda, N. Miura, M. M. Tentzeris, "A Novel Numerical Approach for the Analysis of Ed MEMS – Based Variable Capacitors with Motion to Arbitrary Directions," *The 19^{Th} Annual Rev. of Progress in Applied Computational Electromagnetic*, pp. 48- 53, Monterey March 2003.

[6] A. Dec, K. Suyama, "Micromachined Electro-Mechanically Tunable Capacitors and Their Applications to RF IC's," *IEEE Transactions on Microwave Theory and Techniques,* Vol. 46, No. 12, pp. 2587-2596, December 1998.

[7] A. Dec, K. Suyama, "A 1.9-GHz CMOS VCO with Micromachined Electromechanically Tunable Capacitors," *IEEE Journal of Solid-State Circuits,* Vol. 35, No. 8, pp. 1231-1237, August 2000.

[8] A. Dec, K. Suyama, "Microwave MEMS-Based Voltage-Control Oscillators," *IEEE Transactions on Microwave Theory and Techniques*, Vol. 48. No. 11, pp. 1943- 1949, November 2000

[9] E. S. Hung, S. D. Senturia, "Generating Efficient Dynamical Models for Microelectromechanical Systems from a Few Finite-Element Simulation Runs," *IEEE*

Journal of Microelectromechanical Systems, Vol. 89, No. 3, pp.280-289, September 1999.

[10] *Ansys User Manual*, Ansoft Corp.

[11] R. F. Harrington, *Field Computation by Moment Method*, Mcmillan New York, 1968.

[12] A. E. Ruehli, P.A. Brennan, "Efficient Capacitance Calculations for Three-Dimensional Multiconductor Systems," *IEEE Trans. Microwave Theory and Techniques,* Vol. 21, pp. 76–82, Feb. 1973.

[13] N. Esposito, A. Musolino, M. Raugi "Modelling of three dimensional nonlinear eddy current problems with conductors in motion by an integral formulation", *IEEE Trans. On Magn.* Vol 32, No. 3, pp. 764-767, May 1996.

[14] D. F. Kelley, R. L. Luebbers, "Piecewise Linear Recursive Convolution for Dispersive Media Using FTDT" *IEEE Trans. On Ant. And Prop.,* Vol. 46, No. 6, pp. 792-797, June 1996.

Antonino Musolino was born in Reggio Calabria on January the 7th 1964. He received the Master degree in Electronic Engineering and the Ph. D degree in Electrical Engineering from the University of Pisa in 1990 and 1995 respectively. He is currently an Associate Professor of electrical engineering with the Department of Electrical Systems and Automation, University of Pisa.

His main research activities are the numerical methods for the analysis of electromagnetic fields in linear and nonlinear media, the design of special electrical machines and the application of the WE to computational electromagnetics.

Sami Barmada was born in Livorno, Italy, on November 18, 1970. He received the Master and Ph.D. degrees in electrical engineering from the University of Pisa, Italy, in 1995 and 2001, respectively. From 1995 to 1997, he was with ABB Teknologi, Oslo, Norway, where he was involved with distribution network analysis and optimisation. He is currently an Assistant Professor with the Department of Electrical Systems and Automation, University of Pisa, where he is involved with numerical computation of electromagnetic fields, particularly on the modeling of multiconductor transmission lines and to the application of wavelet expansion to computational electromagnetics. He was the technical chairman of the Progress In Electromagnetic Research Symposium (PIERS), Pisa, Italy, 2004 and has served as chairman and session organizer of international conferences.

Dr. Barmada was the recipient of the 2003 J F Alcock Memorial Prize, presented by The Institution of Mechanical Engineering, Railway Division, for the best paper in technical innovation.

Rocco Rizzo was born in Tricase (Lecce), Italy on August 11, 1971. He received the PhD in Electrical Engineering from university of Pisa in 2002. He is currently an Assistant Professor with the Department of Electrical Systems And Automation, University of Pisa. His primarily area of research is focused on the development of analytical and numerical methods for the analysis of electromagnetic fields in linear and non-linear media, applied to the design of electromagnetic devices for special purposes. In April 2004 he has been elected as a member of Academy of Nonlinear Sciences (ANS) in Russia.